

Implantation of a neoantigen-targeted hydrogel vaccine prevents recurrence of pancreatic adenocarcinoma after incomplete resection

Daniel Delitto^{a,b}, Daniel J. Zabransky^{c,d,e}, Fangluo Chen^{c,d,e}, Elizabeth D. Thompson^{c,d,e,f}, Jacquelyn W. Zimmerman^{c,d,e}, Todd D. Armstrong^{c,d,e}, James M. Leatherman^{c,d,e}, Reecha Suri^{b,c,d,e}, Tamara Y. Lopez-Vidal^{c,d,e}, Amanda L. Huff^{c,d,e}, Melissa R. Lyman^{c,d,e}, Samantha R. Guinn^{c,d,e}, Marina Baretti^{c,d,e}, Luciane T. Kagohara^{c,d,e}, Won Jin Ho^{c,d,e}, Nilofer S. Azad^{c,d,e}, William R. Burns^{b,c,d,e}, Jin He^{b,c,d,e}, Christopher L. Wolfgang^g, Richard A. Burkhart^{b,c,d,e}, Lei Zheng^{b,c,d,e}, Mark Yarchoan^{c,d,e}, Neeha Zaidi^{c,d,e}, and Elizabeth M. Jaffee^{b,c,d,e,f}

^aDepartment of Surgery, Stanford University School of Medicine, Stanford, USA; ^bDepartment of Surgery, Johns Hopkins University School of Medicine, Baltimore, USA; ^cThe Sidney Kimmel Cancer Center, Johns Hopkins University School of Medicine, Baltimore, USA; ^dThe Skip Viragh Center for Pancreatic Cancer Research and Clinical Care, Johns Hopkins University School of Medicine, Baltimore, USA; ^eThe Bloomberg-Kimmel Institute for Cancer Immunotherapy, Johns Hopkins University School of Medicine, Baltimore, USA; ^fDepartment of Pathology, Johns Hopkins University School of Medicine, Baltimore, USA; ^gDepartment of Surgery, New York University Grossman School of Medicine, New York, USA

ABSTRACT

Tumor involvement of major vascular structures limits surgical options in pancreatic adenocarcinoma (PDAC), which in turn limits opportunities for cure. Despite advances in locoregional approaches, there is currently no role for incomplete resection. This study evaluated a gelatinized neoantigen-targeted vaccine applied to a grossly positive resection margin in preventing local recurrence. Incomplete surgical resection was performed in mice bearing syngeneic flank Panc02 tumors, leaving a 1 mm rim adherent to the muscle bed. A previously validated vaccine consisting of neoantigen peptides, a stimulator of interferon genes (STING) agonist and AddaVaxTM (termed PancVax) was embedded in a hyaluronic acid hydrogel and applied to the tumor bed. Tumor remnants, regional lymph nodes, and spleens were analyzed using histology, flow cytometry, gene expression profiling, and ELISPOT assays. The immune microenvironment at the tumor margin after surgery alone was characterized by a transient influx of myeloid-derived suppressor cells (MDSCs), prolonged neutrophil influx, and near complete loss of cytotoxic T cells. Application of PancVax gel was associated with enhanced T cell activation in the draining lymph node and expansion of neoantigen-specific T cells in the spleen. Mice implanted with PancVax gel demonstrated no evidence of residual tumor at two weeks postoperatively and healed incisions at two months postoperatively without local recurrence. In summary, application of PancVax gel at a grossly positive tumor margin led to systemic expansion of neoantigen-specific T cells and effectively prevented local recurrence. These findings support further work into locoregional adjuncts to immune modulation in PDAC.

ARTICLE HISTORY

Received 30 August 2021
Revised 19 October 2021
Accepted 28 October 2021

KEYWORDS

Pancreatic adenocarcinoma;
immunotherapy;
neoantigen; vaccine;
hydrogel; surgery

Introduction


Pancreatic adenocarcinoma (PDAC) is projected to be the second leading cause of cancer deaths by 2030.¹ As with most solid tumors, the only curative intent treatment paradigm involves complete tumor resection. However, at least 30% of patients present with unresectable local disease, involving critical vascular structures for which excision is associated with major morbidity.^{2,3} Given the operative risk combined with the risk of early recurrence, the majority of these patients will not proceed to surgery and are thus ineligible for curative intent therapy.

Advances in locoregional therapies have led to innovative strategies to address locally advanced PDAC (LAPC). These include various forms of intraoperative radiotherapy and irreversible electroporation, both of which have been employed when a threatened margin is anticipated.^{4,5} While conceptually promising, these strategies rely on some degree of selective tissue damage that large blood vessels will theoretically tolerate. However, despite the availability of these tools for over a decade,

concerns over safety and efficacy have limited widespread application. Taken together with conflicting evidence regarding external beam radiotherapy and outcomes, it is safe to conclude that locoregional control remains an elusive goal in LAPC.

The development of immune checkpoint blockade heralded unprecedented advances in immune modulation for cancer therapy. The anchor of this innovation remains rooted in systemic therapy, typically incorporating new systemic combinations with conventional locoregional approaches. However, the implantation of an immunomodulatory agent during surgery remains largely unexplored. Here, we leverage our extensive experience with a pancreatic cancer vaccine to evaluate whether local implantation in a long-acting form might have a role after incomplete tumor resection.⁶⁻⁸ The vaccine components, termed PancVax, were selected after an extensive optimization process involving both the Panc02 neoantigen repertoire and accompanying adjuvants.⁸ Here, we

CONTACT Daniel Delitto Stanford University  delitto@stanford.edu  300 Pasteur Dr, Room H3591, Stanford, CA, 94305, USA

 Supplemental data for this article can be accessed on the [publisher's website](#)

© 2021 The Author(s). Published with license by Taylor & Francis Group, LLC.

This is an Open Access article distributed under the terms of the Creative Commons Attribution-NonCommercial License (<http://creativecommons.org/licenses/by-nc/4.0/>), which permits unrestricted non-commercial use, distribution, and reproduction in any medium, provided the original work is properly cited.

demonstrate that the components of PancVax can be safely implanted as a hyaluronic acid hydrogel during surgery. Further, the application of PancVax gel to a grossly positive tumor margin effectively prevented local recurrence and was associated with systemic expansion of neoantigen-specific T cells.

Materials and methods

Cell culture. The murine Panc02 cell line⁹ was maintained in Dulbecco's Modified Eagle Medium (DMEM, Gibco) supplemented with 10% fetal bovine serum (FBS, Gemini Bio Products), 1% L-glutamine (Gibco) and 0.5% Penicillin/Streptomycin (Gibco) at 37°C with 10% carbon dioxide. Cells were confirmed to be free of mycoplasma prior to experimentation (IDEXX BioAnalytics). Prior to animal injections, cells were suspended with trypsin, counted, and centrifuged. Cells were then resuspended at a concentration of 10 million cells/mL in 50% Matrigel (Corning) and 50% basal media.

PancVax gel generation. Panc02 neoantigens were previously identified and narrowed to 12 consistently immunogenic 20-mer peptides.⁸ Peptides were synthesized by Peptide 2.0 at 95% purity. Lyophilized peptides were dissolved in DMSO at 50 mg/mL and stored at -80°C. HyStem® thiol-modified hyaluronan hydrogel kits (Advanced BioMatrix) were used to generate 300 µL gels allowed to set into a disc shape using sterile 1 cm cloning wells sealed to cell culture plates with sterilized silicone grease. Control gels consisted of 200 µL Glycosil®, 50 µL Extralink® and 50 µL sterile water. In place of sterile water, PancVax gels contained 100 µg 2'3'-c-diAM(PS)2(Rp,Rp) (Invivogen), 50 µL AddaVax™ (Invivogen) and 50 µg of each of the twelve neoantigen peptides. Adjuvant selection was also previously optimized in a flank model of Panc02.⁸ Reagents were mixed into suspension and allowed to set at room temperature for 2 hours.

Animal experiments. Animal experiments were approved by the Animal Care and Use Committee (ACUC) at Johns Hopkins University and conformed to all ACUC safety guidelines. Male 6-week-old C57BL/6 mice were purchased from Jackson Laboratories. Two million Panc02 cells were injected into the subcutaneous tissue overlying the right flank. Tumors were allowed to grow to 1 cm in maximum diameter. At the time of initial resection, an incision was made parallel to the right hindlimb overlying the flank. Tumors were dissected bluntly from the overlying skin and exposed completely down to the muscle. Subcutaneous dissection was kept to a minimum to avoid a large pocket of potential space. Tumors were transected sharply, leaving a 1 mm thick remnant attached to the muscle bed. Hemostasis was achieved with a combination of pressure and cautery. Control or PancVax gels were implanted into the subcutaneous pocket overlying the tumor remnant. The skin was closed with a combination of 3-0 absorbable sutures in a horizontal mattress fashion and surgical clips. At 1, 3, 5, 7, 14 and 60 days postoperatively, the surgical scar was re-explored and the tumor remnant excised with a rim of underlying flank muscle. The right inguinal lymph node and spleen were removed as well. Mice were then euthanized, such that each mouse provided data for a single time point in the postoperative period. Experiments

evaluating PancVax gel were repeated for each group at both 7 and 14 days. For mice undergoing resection with 2 cm tumors, two mice in each group were found to have disease with significant involvement of intraperitoneal structures, precluding safe resection. The analysis was therefore carried out with only 3 mice in each group when tumors regrew to the endpoint size of 2 cm, which occurred on postoperative day 10.

Histology. Murine tumor samples were formalin-fixed and paraffin-embedded by the Johns Hopkins University Oncology Tissue Services. Representative slides were sectioned and stained with hematoxylin and eosin by the Johns Hopkins University Oncology Tissue Services and reviewed by a pathologist experienced in pancreatic disease (EDT).

Flow cytometry. Tumor remnants with surrounding muscle tissue and the right inguinal lymph node basin were separately dissociated into single-cell suspensions using mouse tumor dissociation kits and gentleMACS™ Dissociators according to the manufacturer's protocol (Miltenyi Biotec). Erythrocytes were lysed using ACK Lysing Buffer (Gibco). Single-cell suspensions were stained with one of five optimized panels focusing on NK cells, neutrophils/monocytes, macrophages, B cells and T cells. Cells were incubated with conjugated antibodies in FACS buffer (5% fetal bovine serum in phosphate-buffered saline) for one hour at 4°C. Cells were then washed three times and resuspended in FACS buffer with SYTOX™ Blue (Life Technologies). Cytometry was performed with the CytoFLEX platform (Beckman Coulter). Compensations were set using AbC™ Total Antibody Compensation Bead Kit (Life Technologies). Data were analyzed using FlowJo version 10. Antibodies included the following: FITC conjugated to CD11b and CD3; PE conjugated to NK1.1, Ly6C, F4/80, CD86, and CD137; PerCP-Cy5.5 conjugated to CD69, CD19, and CD45; APC conjugated to NKp46, Ly6G, CD40, CD11c, and CD8; PE-Cy7 conjugated to MHCII and PD1; APC-Cy7 conjugated to CD45 and CD4. All antibodies were specific to mouse antigens and purchased from BioLegend.

NanoString. RNA was isolated from formalin fixed, paraffin-embedded tissue samples from mice one week after resection and gel implantation using the AllPrep DNA/RNA FFPE Kit (QIAGEN) per the manufacturer's protocol. RNA was then analyzed using the Agilent TapeStation 4200, yielding the RNA integrity number (RIN) value and concentration. RIN values were used as inputs into the NanoString FFPE RNA calculator to estimate percentage length. Gene expression analysis was then performed using the nCounter Mouse Immunology Panel. Counts were processed using the nCounter Digital Analyzer and nSolver Analysis Software 4.0. Cell type profiling was performed using methods from Danaher et al.¹⁰ *P* values were adjusted for false discovery rates using the Benjamini-Yekutieli method.

Enzyme-linked immune absorbent spot (ELISPOT). Splenocytes were harvested from mice treated with PancVax gels after incomplete tumor resection on postoperative day 14. Single-cell suspensions were generated by a combination of mechanical lysis and passage through a 40 µm filter. Erythrocytes were lysed using ACK Lysing Buffer. CD4⁺ and CD8⁺ T cells were isolated separately using EasySep™ Mouse CD4⁺ and CD8⁺ T cell isolation kits (STEMCELL

Technologies), respectively, according to the manufacturer's protocol. Five mice from each treatment group were analyzed and T cells were pooled between groups. Multiscreen 96-well filter plates (EMD Millipore) were pre-coated at 4°C for 16 hours with 100 μ L per well of 10 μ g/mL anti-mouse interferon- γ (IFN γ) (Clone AN18, Mabtech). Six technical replicates were performed for each peptide/MHC combination. 10^5 T cells were added to each well followed by 10^5 T2 antigen presenting cells (APCs) after pulsing the APCs with 2.5 μ g/mL of the indicated peptide. T2 APCs were transfected with either H2-K^b, H2-D^b or H2-A^b. Peptides were pulsed with corresponding T2 APCs according to previously established reactivities.⁸ After incubation for 18 hours, cells were discarded and plates were washed. 10 μ g/mL biotinylated anti-mouse IFN γ (Clone R4-6A2, Mabtech) was added to each well for two hours. 3-Amino-9-Ethylcarbazole (AEC) substrate was added for 15 minutes before the reaction was stopped with water. Plates were allowed to sit for one day to dry and counted using an automated ELISPOT reader (ImmunoSpot).

Statistical analysis. Data were analyzed using GraphPad Prism version 8. Groups were compared using 2-tailed, independent samples Student's *t* tests. Statistical significance was considered for $P < .05$.

Results

Development of an incomplete tumor resection model. A model of tumor resection with a grossly positive margin was developed using Panc02 flank tumors. Subcutaneous injections were chosen to minimize any trauma from tumor implantation. At a maximum diameter of 1 cm, tumors were resected to a 1 mm rim of tissue along the muscle bed. Control hydrogels were implanted into the tumor bed and skin flaps closed primarily (Figure 1a). Consistent patterns of tumor regrowth were observed postoperatively, with the development of considerable edema and granulation tissue surrounding the operative site (Figure 1b). Histology confirmed the presence of the hydrogel adjacent to the tumor (Figure 1c) as well as tumor invasion into surrounding muscle and granulation tissue (Figure 1d).

The postoperative immune microenvironment in response to operative trauma and residual tumor. Little is known regarding the evolution of the post-resection immune microenvironment at the site of a positive margin. To better define this, the infiltrating immune landscape at the tumor margin was analyzed in mice implanted with control hyaluronic acid hydrogels after incomplete resection. Expected changes in immune cell

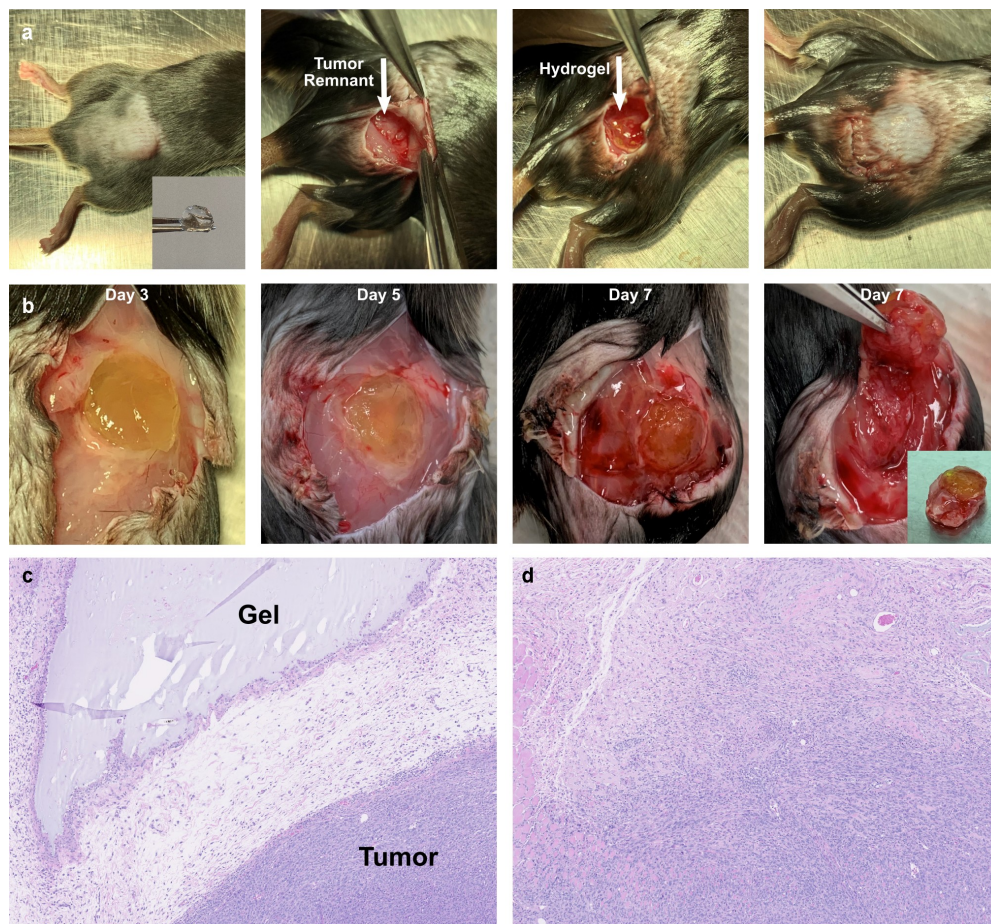


Figure 1. Experimental model of incomplete tumor resection. (a) (Left to right) Panc02 flank tumors were allowed to grow to 1 cm in diameter prior to incomplete resection, leaving a 1 mm rim of tumor on the muscle bed (arrow). A hyaluronic acid hydrogel disc (inset) was implanted adjacent to the tumor bed and the wound closed with sutures and clips. (b) (Left to right) Tumors and surrounding granulation tissue were excised on postoperative day 3, 5 and 7. (Far right) Dissection of the tumor remnant is shown with the final specimen (inset) for either histology or flow cytometry. (c) H&E stain demonstrating the interface between the hydrogel and tumor recurrence. (d) H&E demonstrating tumor regrowth adjacent to postoperative scar and granulation tissue.

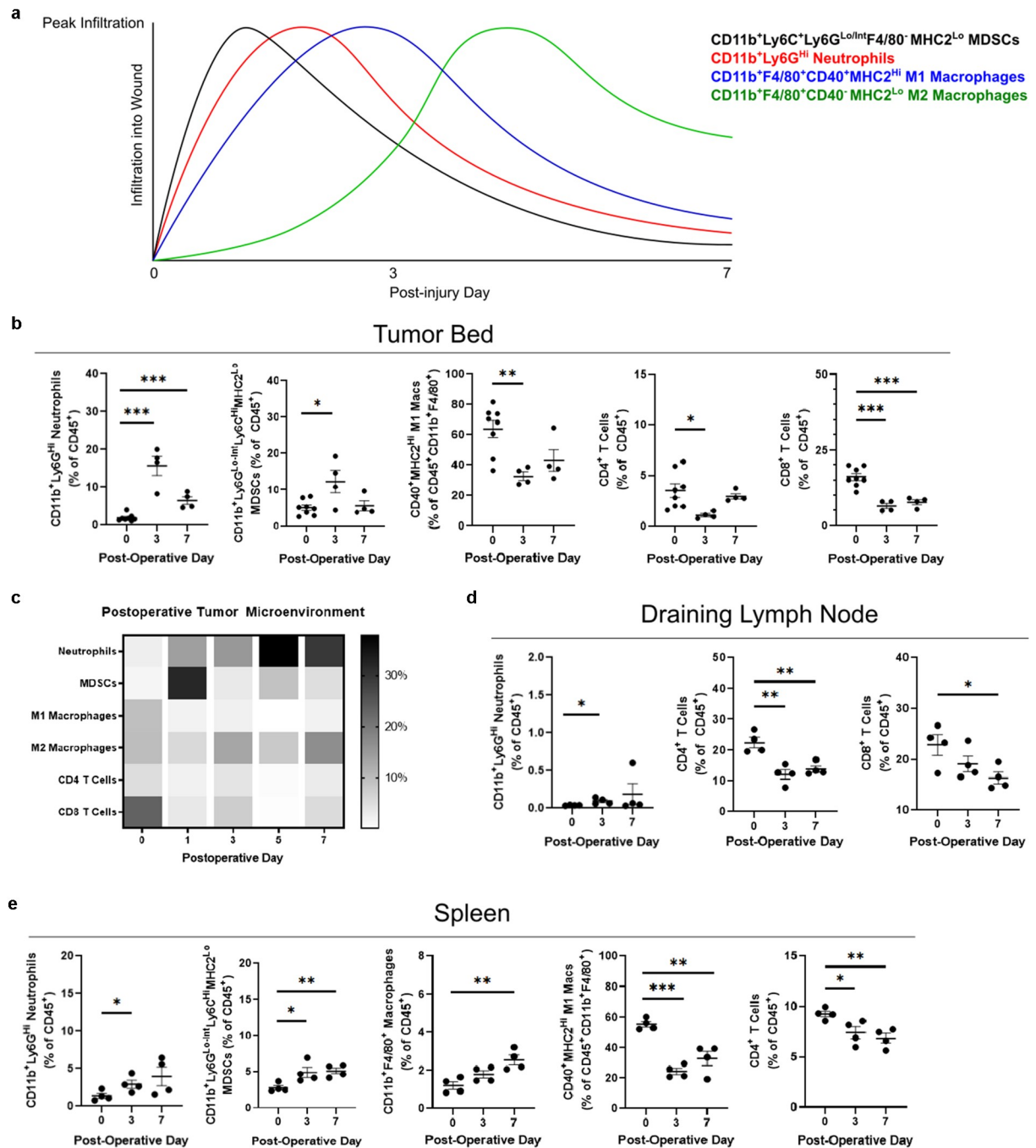


Figure 2. Immunologic changes following incomplete tumor resection. (a) Expected innate immune cell infiltration over the first week of wound healing is approximated from previously published data. (b) Flow cytometry was performed on the digested tumor remnant and surrounding tissue, demonstrating changes in infiltrating myeloid cells and T cells over the first postoperative week. (c) Heat map of immune cell infiltration by each postoperative day in separate experiments. (d) Flow cytometry was performed to analyze immune cell populations in the draining lymph node (right inguinal) and (e) spleen over the first postoperative week. Error bars indicate standard error of the mean. * $P < .05$, ** $P < .01$, *** $P < .001$.

infiltration are approximated in [Figure 2a](#), extrapolated from previous data characterizing skin wounds.^{11–15} In our model, myeloid-derived suppressor cell (MDSC) influx was observed in the early postoperative period that resolved by day 7 ([Figure 2b](#)). Alternatively, neutrophil accumulation followed a longer course, persisting through the end of the first postoperative week ([Figure 2b](#)). While the overall percentage of macrophages did not change, the proportion of CD40⁺MHC2^{Hi} M1-associated macrophages decreased significantly ([Figure 2b](#)). Natural killer (NK) cells similarly did not change by overall

percentage of immune cells, but an increase in the proportion of mature CD11b⁺KLRG1⁺ NK cells was observed ([Figure S1A](#)). Concomitant with an increase in myeloid cells, a striking decline in CD8⁺ T cell presence was observed that did not recover ([Figure 2b](#)). Cell populations that changed significantly through the first postoperative week are displayed together in the heat map in [Figure 2c](#).

In the draining inguinal lymph node basin, a similar increase in neutrophil accumulation was observed, although these cells continued to represent a very small proportion of

the nodal immune component (Figure 2d). A loss of T cells was also observed in the node, predominantly driven by CD4⁺ T cell loss (Figure 2d). In the spleen, diffuse myeloid infiltration was again observed with a similar loss in M1-associated macrophages (Figure 2e). Postoperative day 3 spleens demonstrated a reduction in PD1-positivity for both CD4⁺ and CD8⁺ T cells (Figure S1C). Taken together, these findings confirm a myeloid-rich postoperative immune microenvironment thought to be associated with wound healing. Of note, a persistent reduction of T cells as a fraction of total immune cells was observed in all compartments, suggesting this is unlikely to be a migration phenomenon. T cell populations failed to return to preoperative levels despite significant tumor regrowth, which may have implications for antitumor immune responses in the postoperative period.

Implantation of PancVax gel at the time of resection. In order to test the hypothesis that a hydrogel vaccine would stimulate antitumor immune responses, particularly T cell infiltration, mice were randomly assigned to receive control gels versus PancVax gels upon incomplete tumor resection. Vaccine implantation led to intense neutrophil and MDSC trafficking to the resection bed, with no significant increase in T cells as a fraction of total immune cells (Figure 3a & B). Despite these changes, other encouraging findings regarding antitumor immunity were observed. While the infiltration of NK cells overall was not significantly altered (Figure S1A), the proportion of mature CD11b⁺KLRG1⁺ and activated CD69⁺ NK cells increased with PancVax gel implantation (Figure 3c). In the draining lymph node basin, PancVax gel was associated with CD8⁺ T cell activation in the early postoperative period (Figure 3d) in addition to a similar pattern of NK cell activation to that seen in the tumor bed (Figure 3e). Overall, these data suggest that PancVax gel implantation exacerbated the myeloid infiltration observed with surgery alone at the resection site. In addition, cytotoxic T cell activation in the draining node and global NK cell activation also suggest a potentially favorable environment for an antitumor immune response.

At two weeks postoperatively in the PancVax gel group, persistent neutrophil infiltration was observed in the resection bed, concurrent with an overall reduction in macrophages and NK cells (Figure 4a & B). A slight increase in neutrophils remained present in the draining lymph node, as well as further CD4⁺ T cell loss (Figure 4c & D). In both the lymph node and the spleen, a higher proportion of PD1⁺CD4⁺ T cells was observed in the PancVax gel group (Figure 4c-f). Expression of the co-stimulatory ligand, CD86, was higher in nodal B cells, suggesting more effective antigen presentation in the PancVax gel group (Figure 4d). Higher proportions of multiple myeloid subtypes were present in the spleens of the PancVax gel mice (Figure 4e & F). Consistent with earlier time points, PancVax gel was associated with higher splenic NK cell expression of the activation marker CD69 (figure 4f). Globally, these results suggest persistence of the injury signal from the hydrogel vaccine with release of myeloid cells into the periphery and neutrophil trafficking to the surgical site.

Efficacy of the hydrogel vaccine in preventing tumor recurrence. At one week postoperatively, histologic evaluation revealed uniform regrowth of incompletely resected tumors treated with control hydrogels (Figure 5a). Conversely, mice

treated with PancVax gel demonstrated only scar and granulation tissue with no evidence of tumor in 3 of 5 mice (Figure 5b & C). In the remaining mice, areas of hyalinized necrosis were observed with microscopic deposits of viable tumor cells, which suggests but does not provide definitive evidence of treatment response (Figure 5b & C). At two weeks postoperatively, all mice treated with PancVax gel demonstrated no evidence of tumor at the surgical site (Figure 5d). When the time course was extended to two months postoperatively, all mice treated with PancVax gel demonstrated healed wounds with no evidence of recurrence (Figure 5e). One mouse in this group demonstrated a raised scar at the surgical site, which remained stable in size throughout the 2-month postoperative period. Of note, all timed analyses were performed on separate groups of mice to allow for tissue acquisition at each endpoint. When these experiments were repeated on larger tumors (2 cm), control tumors demonstrated aggressive local recurrence, reaching experimental endpoint in 10 days (Figure S2A). However, mice treated with PancVax gel had no gross evidence of recurrence at this time (Figure S2A). Resection beds again demonstrated similar immune cell infiltration patterns, with a dominant neutrophil and MDSC presence associated with the vaccine (Figure S2B). These experiments provide preclinical evidence for safety and efficacy with PancVax gel application to a grossly positive surgical margin.

Adaptive immune responses to PancVax gel. In order to evaluate whether PancVax gel application led to expansion of neoantigen-specific T cells, interferon- γ ELISPOTs were performed on splenic CD4⁺ and CD8⁺ T cells from experimental mice. Groups included mice undergoing incomplete resection and application of either control gels or PancVax gels at the surgical site. Tumor recurrence was confirmed in the control group and no evidence of tumor confirmed in the vaccine group at two weeks postoperatively. The peptides evaluated consisted of the same 20-mer peptides from the original PancVax validation study⁸ that were also included in PancVax gel. T2 antigen presenting cells expressing either H2-K^b, H2-D^b, or H2-A^b were applied according to previously established peptide reactivity. As the original vaccine was developed to elicit CD8⁺ T cell responses, the majority of neoantigen peptides were designed to maximize binding capacity to H2-K^b or H2-D^b. CD4⁺ T cell responses were also evaluated, since some degree of reactivity has been observed for three of the peptides with H2-A^b. ELISPOTs revealed increased reactivity of CD8⁺ T cells to multiple neoantigen peptides in mice implanted with PancVax gel compared to control gel, suggesting some degree of efficacy as a vaccine despite the traumatized state from surgery (figure 5f). The specific peptides eliciting reactivity were also associated with more pronounced responses in the original PancVax study.⁸ Taken together, these data provide evidence that PancVax gel implantation stimulates neoantigen-specific T cell responses in the postoperative period, concomitant with complete regression of the tumor remnant.

Gene expression profiling of the immune microenvironment after tumor resection and gel implantation. To further explore the nature of immune activity in the resection bed, a panel of 561 genes was analyzed at one week postoperatively using the nCounter NanoString Mouse Immunology Panel. These data

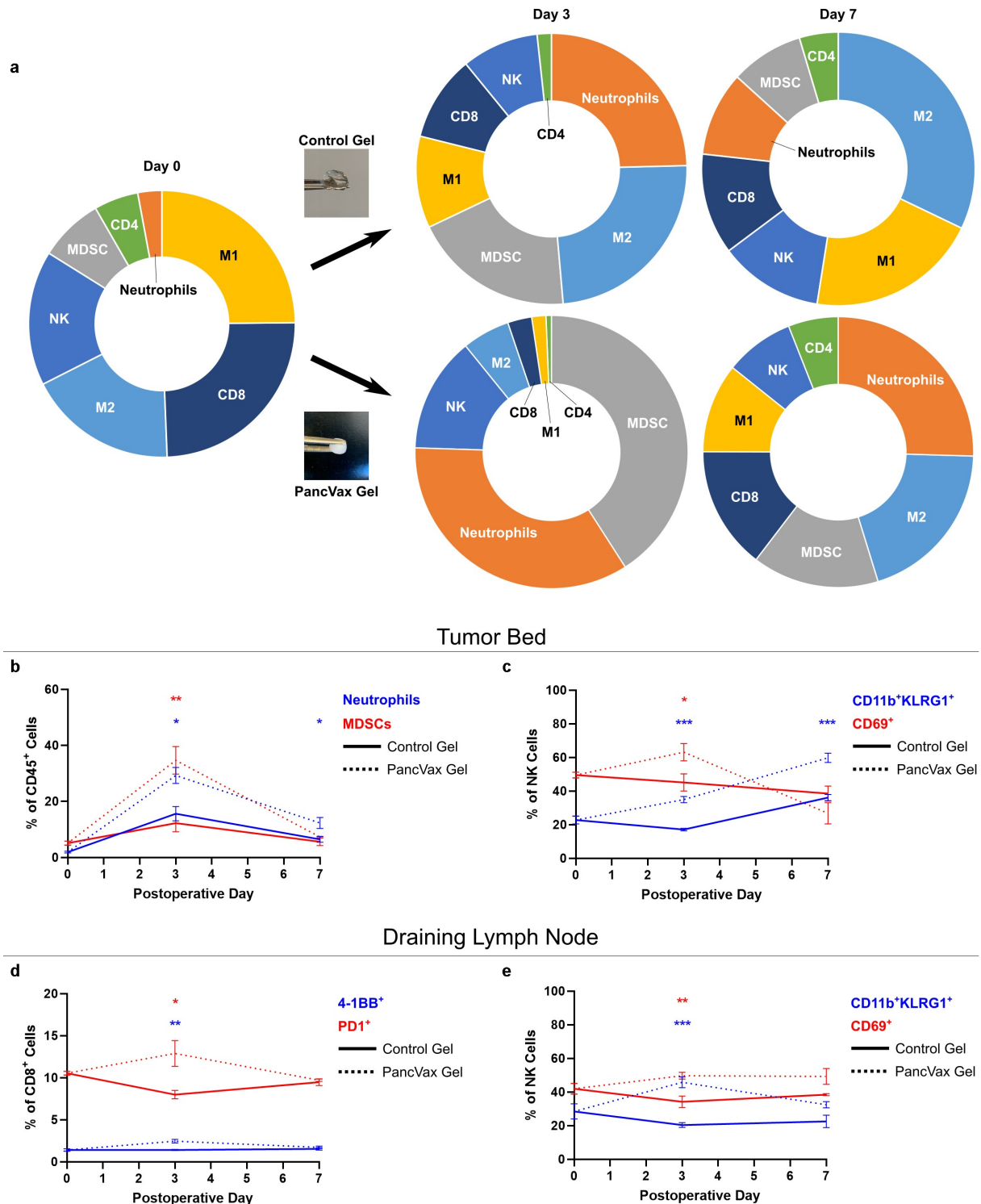


Figure 3. Application of PancVax gel following incomplete tumor resection. (a) Flow cytometry was performed on the digested tumor remnant and surrounding tissue on the indicated postoperative day following incomplete resection and either PancVax gel or control gel implantation. Immune cell breakdown by percentage of CD45⁺ cells is shown in sunburst plots. (b) Neutrophil and MDSC percentages in the tumor remnant are shown over time. (c) NK cell subpopulations are shown in the tumor remnant over time. (d) CD8⁺ T cell activation markers are shown in the draining lymph node (right inguinal) over time postoperatively. (e) NK cell subpopulations are shown in the draining lymph node over time postoperatively. Error bars indicate standard error of the mean. * $P < .05$, ** $P < .01$, *** $P < .001$. Sunburst plots display M1 macrophages in yellow, M2 macrophages in light blue, MDSCs in gray, Neutrophils in Orange, NK cells in royal blue, CD4⁺ T cells in green and CD8⁺ T cells in dark blue.

confirmed the intense innate immune response to PancVax gel, highlighting increased expression of numerous genes associated with granulocyte influx, including S100A8, S100A9, CXCR2, CSF3R, and multiple Fc gamma and pattern-

recognition receptors (Figure 6a-d). Pathway analysis demonstrated enriched signatures associated with both type I and type II interferon signaling, phagocytosis, complement activation, and toll-like receptor signaling (Figure 6e). The PancVax gel

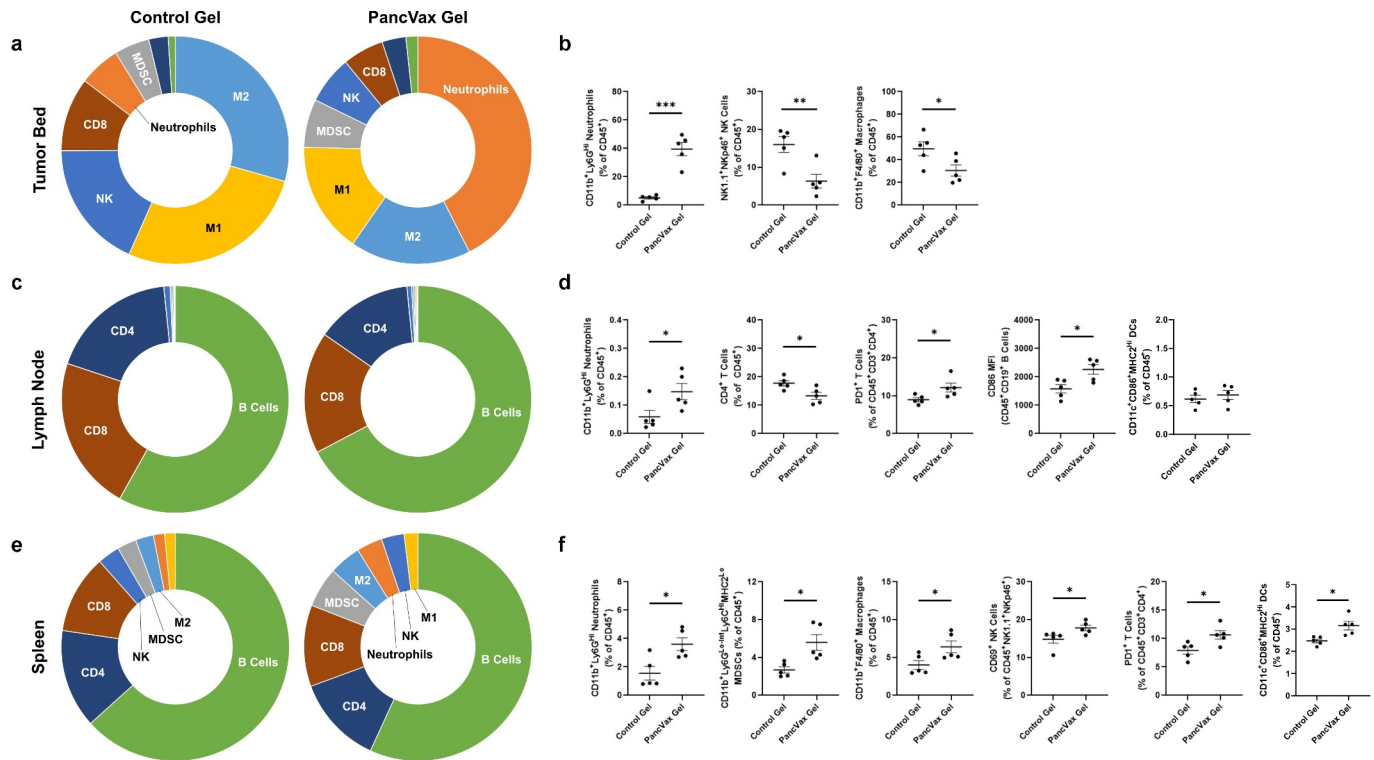


Figure 4. Immunologic changes at two weeks following incomplete tumor resection and PancVax gel application. (a) Flow cytometry was performed on the digested tumor remnant and surrounding tissue on postoperative day 14 following incomplete resection and either PancVax gel or control gel implantation. Immune cell breakdown by percentage of CD45⁺ cells is shown in sunburst plots and (b) selected dot plots. (c) Immune cell breakdown is shown in the draining lymph node (right inguinal) at two weeks following incomplete tumor resection and PancVax gel or control gel implantation in sunburst and (d) selected dot plots. (e) Immune cell breakdown is shown in the spleen at two weeks following incomplete tumor resection and PancVax gel or control gel implantation in sunburst and (f) selected dot plots. Error bars indicate standard error of the mean. * $P < .05$, ** $P < .01$, *** $P < .001$. MFI, mean fluorescent intensity. Sunburst plots display M1 macrophages in yellow, M2 macrophages in light blue, MDSCs in gray, neutrophils in Orange, NK cells in royal blue, CD4⁺ T cells in dark blue, CD8⁺ T cells in brown and B cells in green.

group consistently demonstrated high levels of gene expression associated with phagocytosis and degradation, further reinforcing neutrophil activity and some degree of an M1 macrophage presence (figure 6f). Alternatively, the Th1/Th2 balance favored mice implanted with control gels, suggesting M2-associated activity in the PancVax gel group as well. Interestingly, treatment groups did not cluster together based on gene expression associated with T cell signaling, which included multiple activation markers (Figure 6g). Cell type profiling aligned with flow cytometry data, demonstrating an influx of neutrophils, macrophages and dendritic cells associated with PancVax gel (Figure 6h). All differentially expressed genes are displayed in Table S1. Taken together, these data confirm the innate immune cell influx observed with PancVax gel implantation as well as patterns associated with continued adjuvant activity in the postoperative tumor microenvironment.

Discussion

Implantation of a neoantigen-targeted vaccine embedded in a hyaluronic acid hydrogel (PancVax gel) prevented local recurrence after incomplete tumor resection, leading to durable regression of the gross tumor remnant. PancVax gel application led to T cell activation in the draining lymph node and expansion of neoantigen-specific T cells despite the classically

immunosuppressed postoperative state. To our knowledge, this is the first investigation to demonstrate that locoregional immune modulation at the time of surgery can eliminate residual gross disease.

Our data also describe the temporal changes in the postoperative immune microenvironment after incomplete tumor resection. Traditional wound healing investigations describe an initial phase of inflammation over the first two days, characterized by neutrophil and monocyte recruitment as a result of platelet degranulation, bacterial degradation, chemokine release and a host of other signals.¹⁶ We observed a slightly different pattern of early monocyte recruitment with a prolonged neutrophil presence. While the early monocyte recruitment was not observed in historical wound healing investigations, recent studies using *in vivo* imaging have confirmed an early, “pioneer” wave of monocytes.^{15,17} The persistence of neutrophils surrounding residual tumors compared to the physiologic wound healing process is likely multifactorial. Neutrophil persistence is a known phenomenon in chronic nonhealing wounds, as neutrophil apoptosis is a hallmark event in the transition from the inflammatory to the proliferative phase. Macrophage uptake of apoptotic neutrophils triggers an M2-associated phenotypic change to suppress ongoing inflammation and promote remodeling.^{18–20} However, many of the chemokines and damage associated molecular patterns

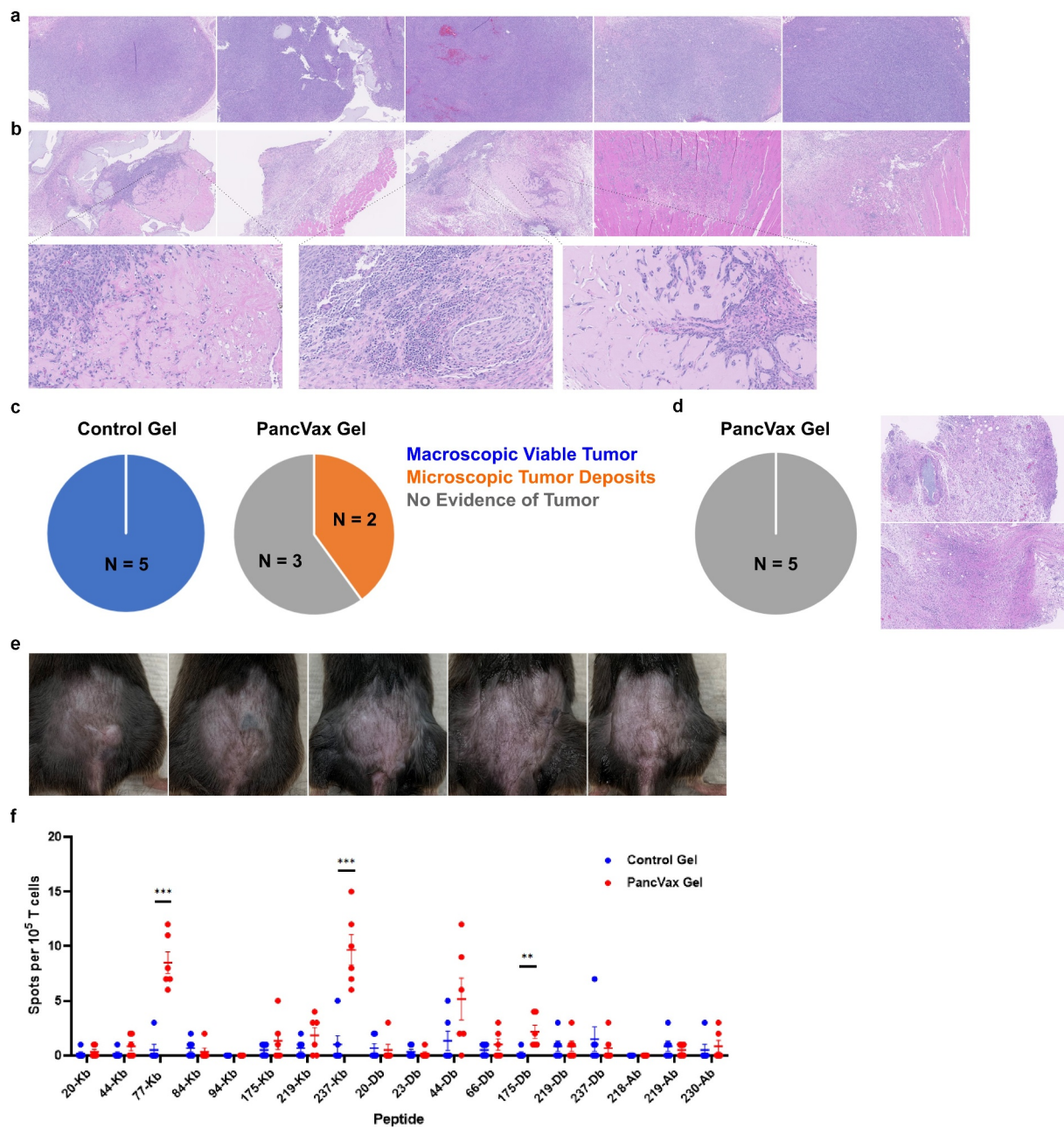


Figure 5. Efficacy of PancVax gel following incomplete tumor resection. (a) H&E analysis of tumor remnants from all mice undergoing incomplete resection with control gel implantation on postoperative day 7. (b) H&E analysis of tumor remnants from mice undergoing incomplete resection and PancVax gel implantation on postoperative day 7 with selected views magnified (20X from 5X). (c) Pie chart summarizing histologic findings from tumor remnants on postoperative day 7 from mice undergoing incomplete tumor resection and the indicated treatment. (d) Pie chart summarizing histologic findings from tumor remnants on postoperative day 14 from mice undergoing incomplete tumor resection and PancVax gel implantation with representative H&E slides demonstrating scar and granulation tissue. (e) Surgical sites of mice undergoing incomplete tumor resection and implantation of PancVax gel on postoperative day 60. (f) Mice undergoing incomplete tumor resection received either PancVax gel or control gel. ELISPOTS were performed to evaluate neoantigen-specific T cell responses. Splensens were harvested on postoperative day 14 and T cells were isolated (CD4⁺ and CD8⁺ separately). T cells were stimulated with T2-D^b or K^b (CD8⁺) or T2-A^b (CD4⁺) antigen presenting cells pulsed with mutant Panc02 peptides identified previously.⁸ Stimulations were performed on an interferon- γ capture plate and spots were counted in an automated fashion (ImmunoSpot).

(DAMPs) known to recruit neutrophils are also abundant in the tumor microenvironment.²¹ Thus, the continued presence of tumor may contribute to the neutrophil persistence observed in our experiments.

Neutrophil recruitment was further exacerbated by the local application of PancVax gel. This may be explained by the immunological context of the new microenvironment. Exposure to the adjuvants in PancVax gel could dramatically alter the physiologic significance of neutrophil apoptosis. As

opposed to the usual tolerogenic stimulus, antigens released from phagocytosed neutrophils may be processed by potential antigen presenting cells in a more hostile context. The resulting cytokine and chemokine release may in turn recruit more neutrophils, providing the framework for a proinflammatory positive feedback loop. Accordingly, the physiologic transition to the anti-inflammatory proliferative and remodeling phases seemed to be delayed in tumor-bearing mice receiving PancVax gel. It is prudent to point out that we cannot rule

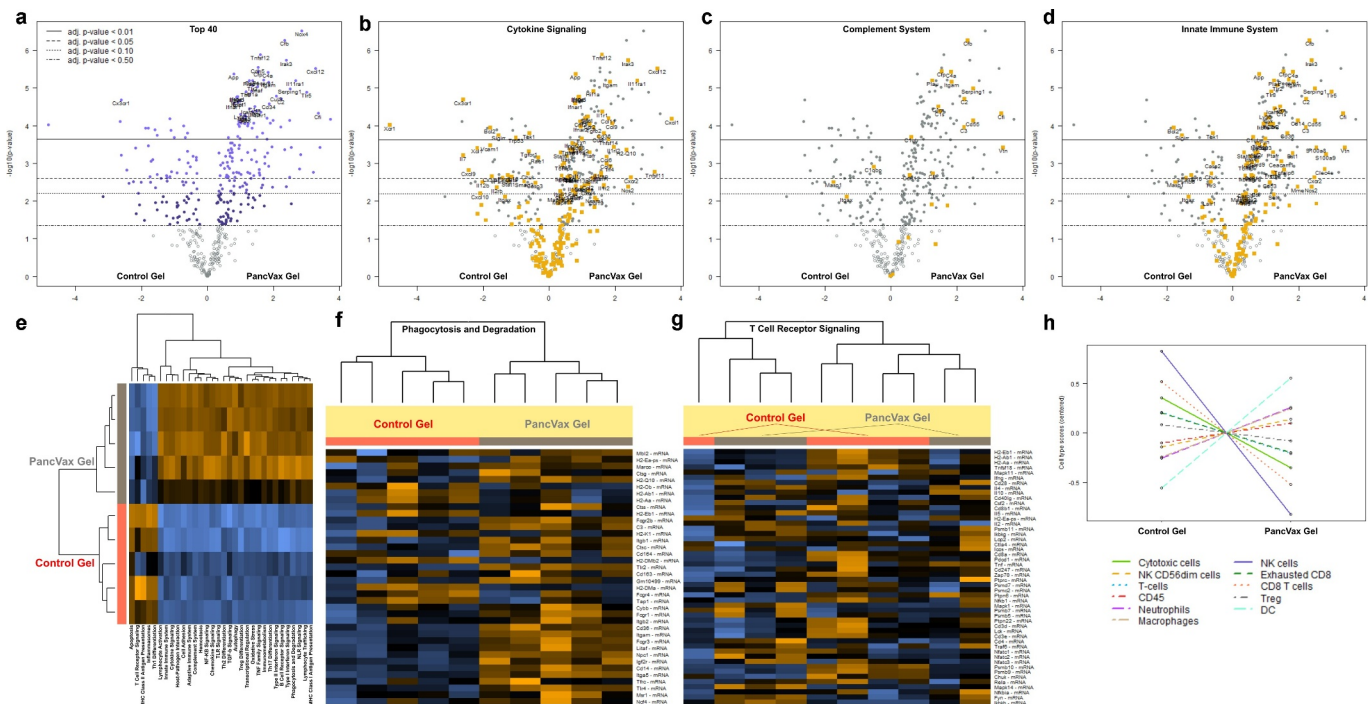


Figure 6. Gene expression analysis of PancVax Gel microenvironment. The NanoString nCounter mouse immunology panel was used to analyze gene expression in the tumor bed one week following resection and gel implantation. Results represent five mice in each group. Volcano plots are displayed highlighting (a) the top 40 differentially expressed genes, (b) genes associated with cytokine signaling, (c) genes associated with complement activation and (d) genes associated with innate immunity. (e) A heat map of the top differentially expressed pathways are displayed for each sample within the treatment groups. (f-g) Heat map analysis of (f) phagocytosis and degradation as well as (g) T cell signaling associated gene expression for PancVax gel samples (gray bar) and controls (red bar). (h) Cell type profiling was performed and differences between groups are displayed. All *P* values were adjusted for false discovery rates using the Benjamini–Yekutieli method.

out a component of granulocytic MDSCs despite very high Ly6G expression. The gene expression data also suggest high phagocytic activity as well as other pathways more consistent with a strong neutrophil presence. Perhaps most importantly, this disruption of the expected wound healing cascade did not appear to impair healing of the incisions in mice receiving PancVax gel.

It is noteworthy that the application of PancVax gel was associated with a higher number of neoantigen-specific T cells despite the global immune suppression from a major operation. While the incomplete resection may appear to be a minor procedure, the proportional area for a mouse is quite large. Further, all mice experienced splenic neutrophil and MDSC accumulation postoperatively, consistent with demargination, arguing in favor of a significant systemic insult. Although the data are sparse, vaccines are generally avoided in the perioperative period due to efficacy concerns. Current guidelines favor vaccination two weeks pre- or two weeks postoperatively for post-splenectomy immunization, the most common perioperative vaccination scenario in adults.^{22,23} While our data suggest that neoantigen-specific T cell expansion and tumor regression can be achieved by an intraoperative vaccine, it is important to recognize that the number of spots observed in this study is well below those observed after injection with PancVax alone.⁸ Further work is necessary to evaluate the expansion of neoantigen-specific T cells in the setting of operative trauma.

Despite neoantigen-specific T cell expansion, the efficacy of PancVax gel did not coincide with a detectable surge in local T cell infiltration. This may be due to the sensitivity of our

methodology, as histologic analysis confirmed that most of the submitted specimen was granulation tissue in the vaccinated mice. Thus, flow cytometry of the entire wound bed may have been biased by the dominant myeloid presence in the surrounding tissue, unable to detect subtle changes in peritumoral T cell influx. Alternatively, the mechanism of efficacy may not be entirely T cell dependent. Intense, persistent neutrophil influx is known to cause significant tissue damage,²¹ which may play a role in sterilizing the resection margins postoperatively. The microenvironment can also have a dramatic effect on macrophage phagocytic function, which can be an effective driver of tumor regression.^{24,25} Gene expression analysis certainly suggested high levels of complement activation and phagocytosis associated with PancVax gel. However, the observations that PancVax gel led to T cell activation in the regional node in addition to neoantigen-specific T cell expansion favor some degree of T cell-mediated antitumor immunity. While expanded analysis of T cell activation markers from the NanoString data also did not detect a significant difference at one week, it is possible that our time points for assessment of T cell activation missed the peak T cell influx period.

Other groups have also demonstrated the potential of vaccines in sustained release formulations. Roth et al generated a polymer-nanoparticle hydrogel-based vaccine that stimulated more effective humoral immune responses.^{26,27} This effect was thought to be the result of prolonged antigen exposure, which led to more extensive somatic hypermutation during affinity maturation. Our methodology was similar to Park et al., who used a hyaluronic acid hydrogel backbone to deliver a variety of immune modulating agents in a highly metastatic 4T1 breast

cancer model.²⁸ This investigation confirmed the release of hydrogel contents over weeks postoperatively and prevention of metastatic disease in a complete tumor resection model. Our study expands on these findings by analyzing a grossly positive tumor margin with an emphasis on local recurrence and the evolving postoperative immune microenvironment, which had not yet been interrogated. Additionally, we applied our established neoantigen-based vaccine, which has already been optimized with the most effective peptide and adjuvant combination.⁸ Unlike the intratumoral injections performed with PancVax previously by our group, no additional systemic agents were necessary to induce regression of the tumor remnant in the PancVax gel model. Data from Park et al. demonstrated significantly worse outcomes with hydrogel placement adjacent to the tumor, supporting the notion that a complete response is exceedingly difficult to achieve without concomitant resection.²⁸ This group also found that adjuvants alone were sufficient to achieve systemic antitumor responses. Future studies with the PancVax gel model will evaluate the contribution of neoantigens to vaccine efficacy in addition to the immune cell types necessary to prevent tumor regrowth.

Here we demonstrate the potential utility of vaccine hydrogels in the operative setting, but these findings should also be considered in the context of several study limitations. First, Panc02 is a PDAC cell line that was examined in a flank tumor model. It should be recognized that both wound healing patterns and vaccine responses may vary depending on the site of injury and vaccine implantation. In PDAC, the major barrier to surgery is often perineural and lymphatic involvement along the mesenteric vessels and portal system. Anticipated margin positivity in these areas represents the ideal application of a vaccine hydrogel, but also entails a unique immune microenvironment that may be difficult to recapitulate experimentally. An orthotopic model is likely more representative of this environment than the flank, but spleen-preserving partial pancreatectomy in a mouse is not technically feasible, particularly with the goal of producing a consistent pattern of local recurrence postoperatively.

Future directions include investigations into tumor rechallenge, oligometastatic disease as well as the application of additional tumor models, as data in PancVax alone is not sufficient to conclude that this represents a clinically viable strategy. In order to maximize consistency, grossly positive margins (R2 resections) were examined rather than microscopically positive margins (R1), which may be more clinically relevant. Experimental endpoints were also preset for consistency in evaluating immunologic changes in the postoperative microenvironment. However, survival analyses will eventually be included in more translational disease models, such as the oligometastatic setting, to ultimately establish the efficacy of this modality. Clinically applicable models will also necessitate incorporation of both male and female mice. As Panc02 was derived in a male mouse, it is our practice to evaluate immunologic phenomena in male mice as well. Additionally, the focus of this study was immune cells in the postoperative tumor microenvironment, but fibroblasts and endothelial cells also comprise a major component of wound healing. Thus, we cannot make conclusions regarding the later stages of neovascularization and fibrosis from these experiments. These data will be important in choosing the appropriate

surgical setting for PancVax gel. Investigations evaluating the safety of PancVax gel may also necessitate more applicable surgical models to PDAC, such as concomitant intestinal or vascular resection. However, despite these limitations, the results at two months suggest both long-term therapeutic efficacy and appropriately healed wounds, representing promising data moving forward.

In summary, we demonstrate the efficacy of an implantable hydrogel vaccine in an experimental model of incomplete tumor resection. Durable tumor regression was observed in the setting of grossly positive margins with locoregional immune modulation alone. Much work remains to further evaluate this approach, but the capacity to effectively treat unresectable local disease would represent a paradigm shift in our approach to solid tumors, particularly PDAC.

Acknowledgments

The authors would like to acknowledge the National Cancer Institute (P01CA247886-01A1 to EMJ, R01CA197296-06 to EMJ and LZ, T32CA126607-11A1 to DD and LZ, K08CA248624-01A1 to NZ, K08CA248710-02 to RAB), the American Society of Clinical Oncology Young Investigator Award (WH), the American Association of Cancer Research Incyte Immuno-Oncology Research Fellowship (WH), the MacMillan Pathway to Independence Award (WH), the Skip Virag Center for Pancreatic Cancer at Johns Hopkins University, the Bloomberg-Kimmel Institute for Cancer Immunotherapy at Johns Hopkins University and the Sidney Kimmel Comprehensive Cancer Center Immune Monitoring Core.

Disclosure statement

WH is a co-inventor of patents with potential for receiving royalties from Rodeo Therapeutics. MY received research grants from Incyte, Bristol-Myers Squibb, Exelixis, and is a consultant for AstraZeneca, Eisai, Exelixis, and Genentech. EJ received a commercial research grant from Bristol-Myers Squibb and Aduro Biotech, and is a consultant and advisory board member for Lustgarten Foundation, Parker Institute for Cancer Immunotherapy, CStone, Dragonfly, Genocera, Achilles and Adaptive Biotechnologies, and co-founder of Abmeta Biotech.

Funding

This work was supported by the American Association for Cancer Research [Incyte Immuno-Oncology Research Fellowship]; American Society of Clinical Oncology [Young Investigator Award]; National Cancer Institute [R01CA197296]; National Cancer Institute [T32CA126607]; National Cancer Institute [K08CA248624]; National Cancer Institute [P01CA247886]; National Cancer Institute [K08CA248710]; National Cancer Institute [T32CA126607]; National Cancer Institute [R01CA197296].

ORCID

Elizabeth M. Jaffee  <http://orcid.org/0000-0003-3841-6549>

References

1. Rahib L, Smith BD, Aizenberg R, Rosenzweig AB, Fleshman JM, Matrisian LM. Projecting cancer incidence and deaths to 2030: The unexpected burden of thyroid, liver, and pancreas cancers in the United States. *Cancer Res.* 2014;74(11):2913–11. doi:10.1158/0008-5472.CAN-14-0155.

2. Gemenetis G, Groot VP, Blair AB, Laheru DA, Zheng L, Narang AK, Fishman EK, Hruban RH, Yu J, Burkhart RA, et al. Survival in locally advanced pancreatic cancer after neoadjuvant therapy and surgical resection. *Ann Surg.* 2019;270(2):340–347. doi:10.1097/SLA.0000000000002753.
3. Suker M, Beumer BR, Sadot E, Marthey L, Faris JE, Mellon EA, El-Rayes BF, Wang-Gillam A, Lacy J, Hosein PJ, et al. Folfirinox for locally advanced pancreatic cancer: a systematic review and patient-level meta-analysis. *Lancet Oncol.* 2016;17(6):801–810. doi:10.1016/S1470-2045(16)00172-8.
4. Krempien R, Roeder F. Intraoperative radiation therapy (IORT) in pancreatic cancer. *Radiat Oncol.* 2017;12(1):8. doi:10.1186/s13014-016-0753-0.
5. Weiss MJ, Wolfgang CL. Irreversible electroporation: a novel therapy for stage III pancreatic cancer. *Adv Surg.* 2014;48(1):253–258. doi:10.1016/j.yasu.2014.05.002.
6. Jaffee EM, Hruban RH, Biedrzycki B, Laheru D, Schepers K, Sauter PR, Goemann M, Coleman J, Grochow L, and Donehower, RC *et al.* Novel allogeneic granulocyte-macrophage colony-stimulating factor-secreting tumor vaccine for pancreatic cancer: a phase I trial of safety and immune activation. *J Clin Oncol.* 2001;19(1):145–156. doi:10.1200/JCO.2001.19.1.145.
7. Zheng L, Ding D, Edil BH, Judkins C, Durham JN, Thomas DL, 2nd, Bever, KM, Mo, G, Solt, SE, and Hoare, JA, et al. Vaccine-Induced intratumoral lymphoid aggregates correlate with survival following treatment with a neoadjuvant and adjuvant vaccine in patients with resectable pancreatic adenocarcinoma. *Clin Cancer Res.* 2021;27(5):1278–1286. 2nd. doi:10.1158/1078-0432.CCR-20-2974.
8. Kinkead HL, Hopkins A, Lutz E, Wu AA, Yarchoan M, Cruz K, Woolman S, Vithayathil T, Glickman LH, Ndubaku CO, et al. Combining sting-based neoantigen-targeted vaccine with checkpoint modulators enhances antitumor immunity in murine pancreatic cancer. *JCI Insight.* 2018;3(20). doi:10.1172/jci.insight.122857.
9. Corbett TH, Roberts BJ, Leopold WR, Peckham JC, Wilkoff LJ, Griswold DP Jr., and Schabel, FM Jr. Induction and chemotherapeutic response of two transplantable ductal adenocarcinomas of the pancreas in C57bl/6 mice. *Cancer Res.* 1984;44(2):717–726.
10. Danaher P, Warren S, Dennis L, D’Amico L, White A, Disis ML, Geller MA, Odunsi K, Beechem J, Fling SP, et al. Gene expression markers of tumor infiltrating leukocytes. *J Immunother Cancer.* 2017;5(1):18. doi:10.1186/s40425-017-0215-8.
11. Joshi N, Pohlmeier L, Ben-Yehuda Greenwald M, Haertel E, Hiebert P, Kopf M, and Werner, S. Comprehensive characterization of myeloid cells during wound healing in healthy and healing-impaired diabetic mice. *Eur J Immunol.* 2020;50(9):1335–1349. doi:10.1002/eji.201948438.
12. Ellis S, Lin EJ, Tartar D. Immunology of wound healing. *Curr Dermatol Rep.* 2018;7(4):350–358. doi:10.1007/s13671-018-0234-9.
13. MacLeod AS, Mansbridge JN. The innate immune system in acute and chronic wounds. *Adv Wound Care (New Rochelle).* 2016;5(2):65–78. doi:10.1089/wound.2014.0608.
14. Strbo N, Yin N, Stojadinovic SO. Innate and adaptive immune responses in wound epithelialization. *Adv Wound Care (New Rochelle).* 2014;3(7):492–501. doi:10.1089/wound.2012.0435.
15. Rodero MP, Licata F, Poupel L, Hamon P, Khosrotehrani K, Combadiere C, and Boissonnas, A. In vivo imaging reveals a pioneer wave of monocyte recruitment into mouse skin wounds. *PLoS One.* 2014;9(10):e108212. doi:10.1371/journal.pone.0108212.
16. Grose R, Werner WS. Wound-Healing studies in transgenic and knockout mice. *Mol Biotechnol.* 2004;28(2):147–166. doi:10.1385/MB:28:2:147.
17. Kim MH, Liu W, Borjesson DL, Curry FR, Miller LS, Cheung AL, Liu, FT, Isseroff, RR, and Simon, SI. Dynamics of neutrophil infiltration during cutaneous wound healing and infection using fluorescence imaging. *J Invest Dermatol.* 2008;128(7):1812–1820. doi:10.1038/sj.jid.5701223.
18. Widgerow AD. Cellular resolution of inflammation–Catabasis. *Wound Repair Regen.* 2012;20(1):2–7. doi:10.1111/j.1524-475X.2011.00754.x.
19. Fadok VA, Bratton DL, Konowal A, Freed PW, Westcott JY, Henson PM. Macrophages that have ingested apoptotic cells in vitro inhibit proinflammatory cytokine production through autocrine/paracrine mechanisms involving tgf-beta, pge2, and paf. *J Clin Invest.* 1998;101(4):890–898. doi:10.1172/JCI1112.
20. Elliott MR, Koster KM, Murphy PS. Efferocytosis signaling in the regulation of macrophage inflammatory responses. *J Immunol.* 2017;198(4):1387–1394. doi:10.4049/jimmunol.1601520.
21. Hua Y, Bergers G, Vs T. Chronic wounds: an immune cell’s perspective. *Front Immunol.* 2019;10:2178. doi:10.3389/fimmu.2019.02178.
22. Howdieshell TR, Heffernan D, Dipiro JT. Therapeutic agents committee of the surgical infection s. surgical infection society guidelines for vaccination after traumatic injury. *Surg Infect (Larchmt).* 2006;7(3):275–303. doi:10.1089/sur.2006.7.275.
23. Shatz DV, Schinsky MF, Pais LB, Romero-Steiner S, Kirton OC, Carlone GM. Immune responses of splenectomized trauma patients to the 23-Valent pneumococcal polysaccharide vaccine at 1 Versus 7 Versus 14 days after splenectomy. *J Trauma.* 1998 discussion 5-6;44(5):760–765. doi:10.1097/00005373-199805000-00004.
24. Barkal AA, Brewer RE, Markovic M, Kowarsky M, Barkal SA, Zaro BW, Krishnan V, Hatakeyama J, Dorigo O, Barkal LJ, et al. Cd24 signalling through macrophage siglec-10 Is a target for cancer immunotherapy. *Nature.* 2019;572(7769):392–396. doi:10.1038/s41586-019-1456-0.
25. Takimoto CH, Chao MP, Gibbs C, McCamish MA, Liu J, Chen JY, Majeti, R, and Weissman, IL. The macrophage ‘do not eat me’ signal, Cd47, is a clinically validated cancer immunotherapy target. *Ann Oncol.* 2019;30(3):486–489. doi:10.1093/annonc/mdz006.
26. Roth GA, Saouaf OM, Smith AAA, Gale EC, Hernandez MA, Idoyaga J, and Appel, EA. Prolonged codelivery of hemagglutinin and a Tlr7/8 agonist in a supramolecular polymer-nanoparticle hydrogel enhances potency and breadth of influenza vaccination. *ACS Biomater Sci Eng.* 2021;7(5):1889–1899. doi:10.1021/acsbomaterials.0c01496.
27. Roth GA, Gale EC, Alcantara-Hernandez M, Luo W, Axpe E, Verma R, Yin Q, Yu AC, Lopez Hernandez H, Maikawa CL, et al. Injectable hydrogels for sustained codelivery of subunit vaccines enhance humoral immunity. *ACS Cent Sci.* 2020;6(10):1800–1812. doi:10.1021/acscentsci.0c00732.
28. Park CG, Hartl CA, Schmid D, Carmona EM, Kim HJ, Goldberg MS. Extended release of perioperative immunotherapy prevents tumor recurrence and eliminates metastases. *Sci Transl Med.* 2018;10(433):433. doi:10.1126/scitranslmed.aar1916.